International Journal of Nanomedicine

Dovepress
open access to scientific and medical research

Open Access Full Text Article

ORIGINAL RESEARCH

Synthesis, Characterization, and Toxicity Assessment of Pluronic F127-Functionalized Graphene Oxide on the Embryonic Development of Zebrafish (*Danio rerio*)

This article was published in the following Dove Press journal:
International Journal of Nanomedicine

Suhaili Shamsi[1]
Addison Alvin Alagan[1]
Seri Narti Edayu Sarchio[2]
Faizah Md Yasin[3,4]

[1]Laboratory of Animal Biochemistry and Biotechnology, Department of Biochemistry, Faculty of Biotechnology and Biomolecular Sciences, Universiti Putra Malaysia, Serdang, Selangor 43400, Malaysia; [2]Department of Biomedical Sciences, Faculty of Medicine and Health Sciences, Universiti Putra Malaysia, Serdang, Selangor 43400, Malaysia; [3]Department of Chemical and Environmental Engineering, Faculty of Engineering, Universiti Putra Malaysia, Serdang, Selangor 43400, Malaysia; [4]Institute of Advanced Technology, Faculty of Engineering, Universiti Putra Malaysia, Serdang, Selangor 43400, Malaysia

Background: In the current literature, there are ongoing debates on the toxicity of graphene oxide (GO) that demonstrate contradictory findings regarding its toxicity profile. As a potential drug carrier, these findings are very concerning due to the safety concerns in humans, as well as the dramatic rise of GO being excreted into the environment. Therefore, there is an imperative need to mitigate the potential toxicity of GO to allow for a safer application in the future.

Purpose: The present study aims to address this issue by functionalizing GO with Pluronic F127 (PF) as a means to mitigate toxicity and resolve the biocompatibility of GO. Although results from previous studies generally indicated that Pluronic functionalized GO exhibits relatively low toxicity to living organisms, reports that emphasize on its toxicity, particularly during embryonic developmental stage, are still scarce.

Methods: In the present study, two different sizes of native GO samples, GO and NanoGO, as well as PF-functionalized GO, GO-PF and NanoGO-PF, were prepared and characterized using DLS, UV-Vis, Raman spectroscopy, FTIR, and FESEM analyses. Toxicological assessment of all GO samples (0–100 μg/mL) on zebrafish embryonic developmental stages (survival, hatching and heart rates, and morphological changes) was recorded daily for up to 96 hours post-fertilization (hpf).

Results: The toxicity effects of each GO sample were observed to be higher at increasing concentrations and upon prolonged exposure. NanoGO demonstrated lower toxicity effects compared to GO. GO-PF and NanoGO-PF were also found to have lower toxicity effects compared to native GO samples. GO-PF showed the lowest toxicity response on zebrafish embryo.

Conclusion: These findings highlight that toxicity is dependent on the concentration, size, and exposure period of GO. Functionalization of GO with PF through surface coating could potentially mitigate the toxicity effects of GO in embryonic developmental stages, but further investigation is warranted for broader future applications.

Keywords: graphene oxide, pluronic, nanomaterial, toxicity, embryogenesis

Correspondence: Suhaili Shamsi
Laboratory of Animal Biochemistry and Biotechnology, Department of Biochemistry, Faculty of Biotechnology and Biomolecular Sciences, Universiti Putra Malaysia, Serdang, Selangor 43400, Malaysia
Tel +603-9769 7964
Fax +603-9769 7590
Email sh_suhaili@upm.edu.my

Introduction

Nanotechnology has paved the way for the creation of new tools which could solve many longstanding global issues currently being faced by mankind. In recent years, new discoveries and advances in the field of nanotechnology has spurred renewed interests of its potential applications in various disciplines such as engineering,

submit your manuscript | www.dovepress.com
DovePress
http://doi.org/10.2147/IJN.S271159

biotechnology, as well as biomedicine. This has only been possible in recent decades which saw many notable ground-breaking discoveries being made that ultimately sparked the rapid expansion of research in this relatively new field of science. Today, nanotechnology has become one of the most promising research areas with numerous novel discoveries in journal publications and its myriad of exciting applications. At its core, the field of nanotechnology revolves around nanomaterials or nanoparticles and at the forefront of this new age of nanomaterial research are graphene-based nanomaterials.

Graphene is a carbon-based compound that consists of a single or multi-layered sheet of graphitic films that are made up of a honeycomb-shaped lattice structure with a thickness of approximately 1 nm.[1] It has also been established to be one of the stable materials and has been dubbed the "wonder material" with myriad of applications, especially in the field of biomedicine.[1] Graphene oxide (GO), a derivative compound of graphene, is produced by oxidation process which introduces oxygenated functional groups in the graphene structure. This highly oxidized structure imparts hydrophilic properties on the basal planes and edges that allow GO to be more stable in water suspensions and, hence, more easily exfoliated into monolayer sheets.[2] The basal planes of GO also possess hydrophobic properties due to the presence of free surface π electrons which allows π–π interactions to occur for drug loading.[3] Thus, the amphiphilic properties of GO sheet-like molecule help to stabilize hydrophobic molecules such as poorly water-soluble drugs without affecting its therapeutic efficacy.[4] Previous studies on GO highlight a possible therapeutic application as an anti-microbial agent due to its potential anti-microbial activity against gram-negative and gram-positive bacteria.[5–7] GO can also be conjugated with other compounds that possess pharmacological activity as well as a potential candidate for a targeted drug delivery system for cancer therapy. Previous researches utilized anti-cancer drugs, doxorubicin (DOX) and camptothecin (CPT) as a drug model in a GO nanocarrier study.[8–10]

However, with the potential application of GO as a drug carrier, the safety concerns of GO have been brought up. As recent studies have demonstrated, the toxicity profile of GO in a number of in vitro and in vivo systems has been elusive. In current literature, there are ongoing debates on the toxicity of GO which is also reflected in the journal publications that demonstrate somewhat contradictory findings regarding its toxicity profile. As a potential drug carrier, these findings are very concerning due to safety concerns in humans, as well as the dramatic rise of GO being inevitably excreted into the wastewater and subsequently, the environment. Based on previous study, GO has the ability to penetrate the plasma membrane and potentially alter the cell morphology and ultimately induce cell apoptosis.[11,12] In addition, in vivo studies also demonstrated chronic toxicity in mice exposed to high concentrations of GO, with signs of chronic toxicity observed in the lungs and liver of surviving mice.[13,14]

Therefore, there is an imperative need to look into ways to mitigate the potential toxicity of GO to allow for a safer application and more effective disposal of GO in the future. Surface coating or surface functionalization could be a promising solution to reduce the toxicity of GO, as reported by previous studies (Table 1), which utilized polyethylene glycol (PEG),[15] poly (amido amine) (PAMAM),[16] and dextran (DEX).[17] Reduced toxicity of GO conjugated with polymers, such as polyethylene glycol (PEG) and dextran (DEX),[18] has been reported in A549 human cells. A previous study by Ma et al[19] has reported that GO coated with Pluronic (GO-MB/PF127) was highly biocompatible towards HL-7702 normal liver cell line, with cell viability remaining greater than 90% even at concentrations up to 10 μg/mL after 48 hours and 72 hours of exposure. In addition, an in vitro study conducted using GO dispersed with Pluronic has shown that Pluronic could improve GO biocompatibility in fibroblast cells, with only 5% of inhibition towards cell proliferation at concentrations of up to 50 μg/mL for 72 hours, which

Table 1 Biocompatibility of Surface Functionalized GO

Surface Coating	Findings	References
Polyethylene glycol (PEG)	GO shows no toxicity towards J774A.1 murine macrophage cell line at concentrations up to 100 μg/mL at 24 hours of exposure	Xu et al 2018[15]
Poly (amido amine) (PAMAM)	GO shows good biocompatibility to the SMMC-7721 human hepatocarcinoma cells with 93% viability at a concentration of 200 μg/mL upon 24 hours of exposure	Liu et al 2018[16]
Dextran	Highly compatible, no toxicity up to 450 μg/mL (80% viability) in HeLa human cervical carcinoma cells	Kim et al 2011[17]

was an improvement of more than 50% in cell viability.[20] This demonstrates that Pluronic significantly modifies the biocompatibility of GO by affecting the intracellular interaction and penetration of GO. Although results from previous studies generally indicate that Pluronic functionalized GO exhibits relatively low toxicity to living organisms, reports that emphasize its toxicity, particularly during embryonic developmental stages, are still scarce. Embryonic developmental stage is an important phase in life and any disruption towards this stage could bring various deleterious effects and diseases. Therefore, the present study aims to address this issue by evaluating the toxicity of Pluronic-functionalized GO on zebrafish embryogenesis.

Zebrafish as a model organism has attracted the interest of many researchers due to its unique characteristics, which are small size, transparent, and short breeding cycle that promote high throughput chemical screening.[21] In addition, 70% of zebrafish genes have been found to be homologous to human genes and it also exhibist similar physiology responses, especially during the development of chronic diseases.[22] Apart from that, zebrafish embryos are structurally and functionally similar to humans, with a protruding yolk sac that supplies micronutrients and vital biomolecules such as protein and lipid for a sustained metabolic function and growth until the onset of exogenous feeding in zebrafish, or placental–fetal exchange in humans.[23] Thus, the present study investigated the toxicity effects of two different sizes of GO and evaluated the functionalization of GO with Pluronic as a means to mitigate toxicity and resolve the biocompatibility of GO in a zebrafish embryonic model.

Materials and Methods

Materials

Graphite powder was purchased from ThermoFisher Scientific. Sulphuric acid (PP: 98%, AR), phosphoric acid (H_3PO_4) (PP: 85%, AR), hydrogen peroxide (H_2O_2) (PP: 30%, AR), hydrochloric acid (HCl) (PP: 37%, AR), ethyl alcohol (PP: 99.8%, AR), diethyl ether, and potassium permanganate powder ($KMnO_4$) were obtained from R&M chemicals. Triblock copolymers Pluronic® F127 was purchased from Sigma-Aldrich (St Louis, MO, USA). All experiments were conducted using deionized water.

Synthesis of Graphene Oxide (GO)

An improved Hummers method[24] was used to synthesize GO using graphite powder. A 9:1 mixture of concentrated H_2SO_4/H_3PO_4 (360:40 mL) was added to a mixture containing 3.0 g graphite powder. While stirring, 18 g of $KMnO_4$ was added gradually to the above reaction mixture, at the temperature of 40°C. Then, the mixture was heated up to 50°C and stirring was continued for 12 hours. The reaction mixture was cooled to room temperature for 2 hours and poured into an ice bath (400 mL) with the addition of 3 mL of H_2O_2. A centrifugation technique (Sorvall, USA) at 4000 rpm was used to decant the supernatant from the mixture above. The suspension was washed in succession with 200 mL of distilled water, 200 mL of HCL, and 200 mL of ethanol to remove any impurities. The suspension obtained was vacuum filtered using PTFE membrane (50 nm of diameters and 0.45 µm pore size) (Sigma-Aldrich, USA) and left to dry overnight at room temperature.

Preparation of Graphene Oxide (GO) at Different Sizes

Based on a method outlined by Hu et al,[25] two different samples of native GO with different sizes, GO and NanoGO, were prepared accordingly. To prepare micro-sized GO, 0.015 g of GO powder was dispersed in 15 mL of deionized water by bath sonication (60 W, 40 kHz) (Skymen, China) for 5 minutes. Next, GO dispersion was left to stir overnight (Heidolph MR3001K, Germany) to obtain a more uniform and well dispersed solution. To prepare nano-sized GO (NanoGO), 0.015 g of GO powder was dispersed in 15 mL of deionized water and was subjected to bath sonication (60 W, 40 kHz) (Skymen, China) for 24 hours to produce nano-sized GO particles.

Preparation of Pluronic-Functionalized Graphene Oxide at Different Sizes

Two different samples of Pluronic F127 (PF)-functionalized GO with different sizes, GO-PF and NanoGO-PF, were also prepared according to Hu et al.[25] Then, 0.4 g of Pluronic powder was added gradually into the GO dispersion and stirred for 24 hours to produce GO-PF dispersion. To prepare NanoGO-PF, the GO-Pluronic mixture was sonicated for 24 hours to produce NanoGO-PF. Lastly, any excess Pluronic (unbound Pluronic) was removed using dialysis (Spectra/Por® 7 Dialysis Membrane, MWCO: 12–14 kDa,

CA, USA) against 2 L of water over 2 days, with water replacement every other day.

Physicochemical Characterization

The Raman spectroscopic analysis of GO and NanoGO samples was conducted using a "Wissenschaftliche Instrumente und Technologie" (WITec) Raman spectrometer, Alpha 300R (WITec GmbH, Ulm, Germany). The Raman frequency was acquired with a laser excitation wavelength of 532 nm and an integration time of 5.03645 (s). The laser power on the sample was kept low to avoid heating effects. The surface functional groups of the GO, NanoGO, GO-PF, and NanoGO-PF were investigated using Fourier transform infrared spectroscopy (FTIR-attenuated total reflection mode) technique using the Thermo Nicolet Model, Nicolet 6700 (Thermo Scientific, Waltham, MA, USA). No sample preparation was needed for the ATR method. The sample was placed on the stage, enough to cover the diamond area. Each disc was scanned at a resolution of 4 cm^{-1} over a frequency region of 400–4,000 cm^{-1}. Each spectrum represents an average of 32 scans. The X-ray diffraction (XRD) patterns were obtained at 30 kV and 30 mA, with a scanning rate of 2°/min and 2 Θ angles ranging from 2–60° with an XRD-600 Diffractometer (Shimadzu, Tokyo, Japan). The surface morphology and elemental analysis of all GO, NanoGO, GO-PF, and NanoGO-PF were observed using a field-emission scanning electron microscope (FESEM) (FEI, USA) equipped with an EDX spectrometer by placing 5 µL of the samples on an aluminium stub and then drying overnight at room temperature. High resolution TEM (HRTEM) imaging of GO and NanoGO was examined under a Hitachi H-7100 TEM equipped with a thermionic tungsten source operating at 200 kV. Samples were diluted with acetone and allowing the diluted dispersions to dry at ambient temperature overnight on 200 mesh carbon-coated copper TEM grids.

The electronic structures of GO, NanoGO, and NanoGO-PF were assessed by a UV-Vis spectrophotometer (Jenway 7315 Spectrophotometer, USA). Absorption spectra were registered in the range of 200–800 nm. The particle hydrodynamic diameter, size distribution, and zeta potential (surface charge) of GO, NanoGO, GO-PF, and NanoGO-PF were assessed by using a Malvern Zetasizer Nano ZS instrument (Malvern Instruments, Malvern, UK) equipped with a 633 nm He-Ne laser operating at an angle of 173°. Disposable cuvettes DTS1070 (folded capillary zeta cells) were used for experiments with a sample volume of 1 mL. All measurements were carried out using water as a solvent using a refractive index (n=1.330), dielectric constant=78.5, and viscosity at 25°C=0.8872 cP. Three independent measurements were averaged, performed at controlled temperature (25°C), with an automatic attenuator for each sample.

Toxicity Assessment on Zebrafish Embryos

The Danio Assay Kit for toxicity assessment was purchased from the Danio Assay Laboratories (Danio Assay Laboratories Sdn. Bhd, UPM, Malaysia), which was equipped with live zebrafish embryos, 96 well plates, 500 mL of Danio-embryo media containing 0.1% DMSO, and manual instruction. The wild-type Zebrafish (AB strain) was maintained by the Danio Assay Laboratories according to standard in a recirculation system, and under the permission of the Institutional Animal Care and Use Committee (IACUC), Universiti Putra Malaysia (UPM/IACUC/AUP No. R024/2014). Any dead/coagulated embryos that appeared milky, white, and opaque were separated from the healthy embryos and discarded. Next, the old medium in the petri dish containing the embryos was removed and replaced with fresh embryo media that was provided with the Danio Assay Kit. The embryos were then carefully transferred into a 96-well plate with one embryo per well. The embryos in the plate were incubated overnight at 28±2°C with a 10-hour light/14-hour dark cycle to allow the embryos to acclimatize to the environmental/laboratory conditions. Toxicity assay was performed for all four GO dispersions. At 24 hours post-fertilization (hpf), each embryo was treated with different concentrations of each GO dispersion (0–100 µg/mL) and deionized water as control (n=3, with eight embryos per each replicate).[26] The embryonic development was assessed daily for survival rate, heart rate, hatching rate,and malformations during each observation (24 hpf to 96 hpf). The heartbeat was observed clearly under an inverted microscope and recorded manually by using a stopwatch for a duration of 15 seconds. The number of heartbeats counted was multiplied by four to obtain the heart rate as beats per minute (bpm).[27] Furthermore, the hatching rate of zebrafish embryos was also observed and recorded as "1" to indicate hatched embryo, while for a non-hatching embryo it was recorded as "0". Embryos were observed under an inverted microscope to assess the survival rate. Embryos were considered as dead/coagulated when the embryos appeared milky white, opaque with visible cellular degeneration, as

well as presence of total or partial unrecognizable structures. The absence of any sign of heartbeat during 15 seconds of observation was also considered as the embryo being dead. Each embryo that was observed as dead or coagulated was recorded as "1", while embryos that survived were recorded as "0" in the data collection sheet of each toxicity assay.

Assessment of morphological development along with any underlying abnormalities was observed for each treated embryo. Each embryo was observed at 24 hours interval (24 hpf to 96 hpf). The embryos were examined by using a TS100 inverted microscope at 40X magnification (Nikon, Japan). Several parameters of morphological development, such as the presence of body curvature or scoliosis, edema formation, non-detachment of tail, and lack of somite formation were observed to assess any abnormalities in the treated embryos. An image of each embryo was captured using a DinoLite microscope camera attached to an inverted microscope. The DinoLite microscope camera was operated through a DinoCapture 2.0 software interface that was installed on a laptop (Dino-Lite, USA). All morphological observation data was recorded as "1" to indicate malformation in the data collection sheet while a healthy embryo without any signs of malformation was recorded as "0". This was recorded for each developmental parameter previously mentioned above.

Statistical Analyses

Statistical analysis was performed using SPSS 16.0 (SPSS Inc., Chicago, IL, USA). Particle size, size distribution, and zeta potential data were analyzed by one-way ANOVA (Analysis of Variance) with post hoc Tukey's test applied for paired comparison of means. One-way ANOVA was also used to determine the significance of toxicity effects at different concentrations of each GO dispersion exposure as compared to the respective control group. After ANOVA was performed, Tukey and Dunnet post hoc test was used to compare between exposure groups with control. Data are presented as the mean±standard deviation and the data were significant when the P-value was ≤ 0.05.

Results and Discussion

Raman Spectroscopy

Raman spectroscopy is a non-destructive technique that has been widely employed for the characterization of carbon-based structures such as GO nanoparticles. This is due to the fact that conjugated and double carbon–carbon bonds present in GO structures lead to high Raman intensities. The Raman spectrum provides useful information on defects, carbon sp^2 vibrations, and the stacking order. The G and D bands are attributed to the first-order scattering from the E2g photon of sp^2 carbon bonding and structural defects (disorder-induced modes), respectively.[28] Pristine graphite consists of a single layer of sp^2 hybridized carbon atoms arranged in a honeycomb lattice structure. On the other hand, GO is a highly oxidized graphene consisting of oxygenated functional groups such as hydroxyl, epoxy, carbonyl, and carboxyl groups that contribute to the formation of sp^3 domains clustered throughout the crystal lattice. In the Raman spectra of NanoGO (Figure 1), there was a broaden graphite lattice (G band) at 1604 cm^{-1} and a structural disorder band caused by the graphite edges (D band) at approximately 1365 cm^{-1}. The G-band positions shifts to higher frequencies from 1594 cm^{-1} to 1604 cm^{-1} after oxidation,[29] and the D-band shifts from 1354 cm^{-1} to 1365 cm^{-1} in NanoGO compared to GO. This phenomenon can be attributed to the changes of the GO lattice structure, when GO is exfoliated upon 24 hours of sonication.[30] The enhancement of ID/IG ratio correlated with the level of defects and disorders of GO sheets. However, the ratio of ID/IG intensity of GO (0.850) and NanoGO (0.851) does not differ significantly.

Fourier Transform Infrared Spectroscopy

As shown in Figure 2A, the FTIR spectra present oxygen functionalities groups in where a strong absorption band was

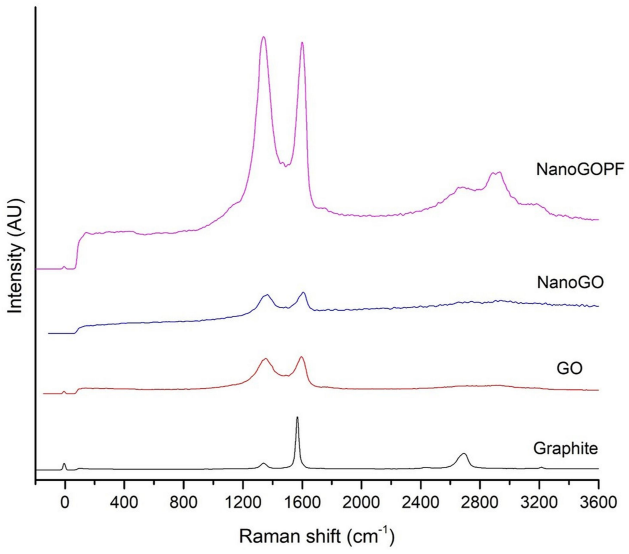

Figure 1 Raman spectra of GO and NanoGO samples obtained using 532 nm diode laser excitation.

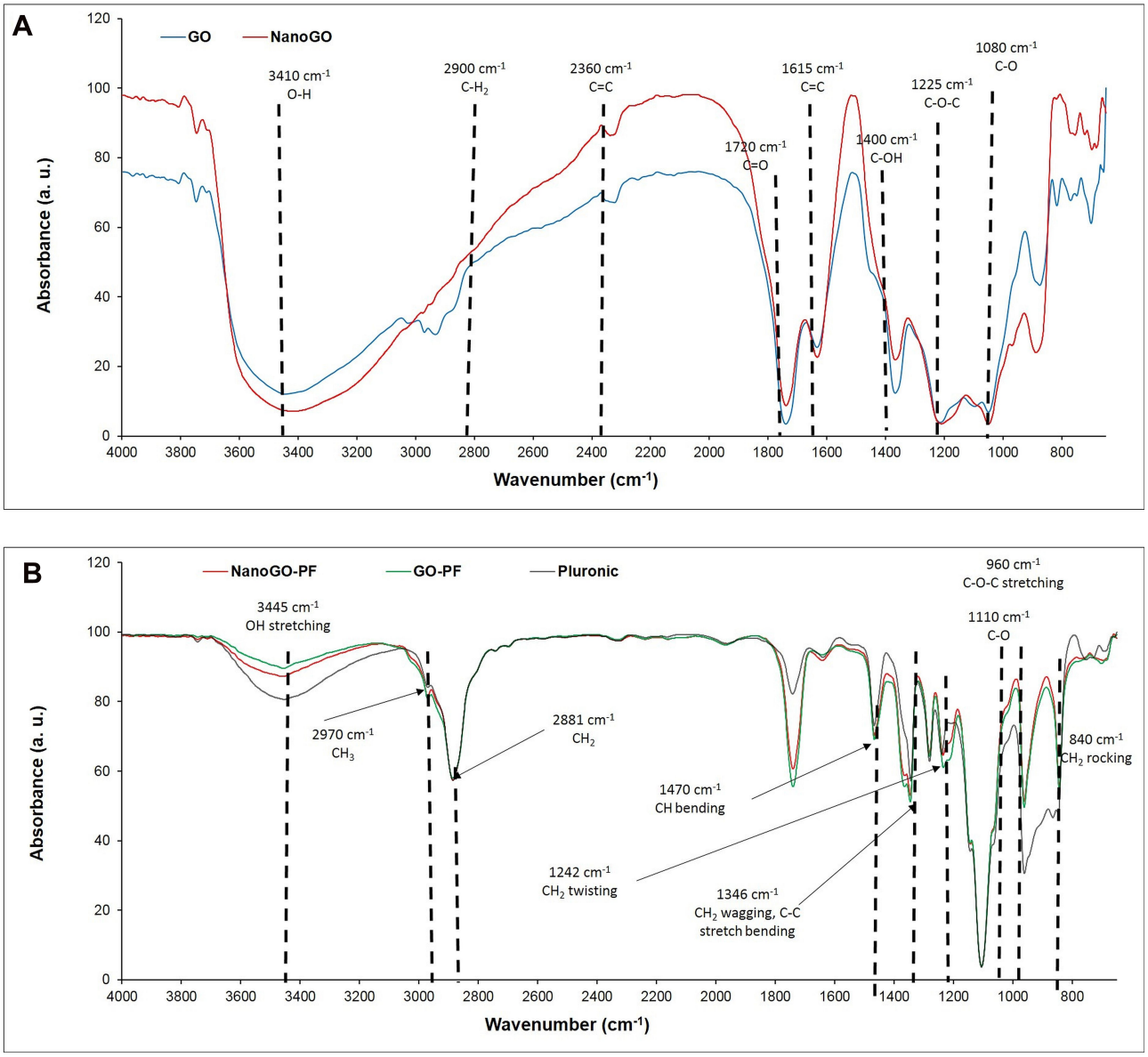

Figure 2 FTIR spectra of: (**A**) GO and NanoGO samples; and (**B**) GO-PF, NanoGO-PF, and PF.

observed at 3,172 cm^{-1} (O-H stretching vibrations), 1,725 - cm^{-1} (C=O stretching vibrations).[31] Bands at 1,621 cm^{-1} (C=C skeletal vibrations from unoxidized graphitic diamonds), 1,155 cm^{-1} (epoxy C-O stretching), and 1,042 cm^{-1} (alkoxy C-O stretching vibrations) were observed in GO.[32] After the sonication of GO, which produced the NanoGO derivative, the intensities for the spectra observed at 3,227 - cm^{-1} (O-H stretching vibrations), 1,717 cm^{-1} (C=O stretching vibrations), 1,621 cm^{-1} (C=C skeletal vibrations from unoxidized graphitic diamonds), 1,158 cm^{-1} (epoxy C-O stretching), and 1,035 cm^{-1} (C-O stretching vibrations) are slightly weak. Thus, the data above confirms that no significant change in the functional groups was observed between GO and NanoGO. Interestingly, FTIR spectra of GO-PF and NanoGO-PF (Figure 2B) share an almost identical spectrum with Pluronic which supports the assertion that successful functionalization of GO with Pluronic has occurred. Pluronic was bound to GO and formed a surface coating which covered the underlying functional groups that were characteristically present in GO samples. As can be seen in Figure 2B, a strong absorption peak at 3,450 cm^{-1} is attributed to the O-H bond stretching, which has dramatically decreased in GO-PF and NanoGO-PF samples. This is coupled with the decrease in the characteristic peak at 1,730 - cm^{-1}, corresponding to C=O bond vibration, indicative of the fact that most of the oxygen-containing functional groups

was not detected on the GO structure, which implies that Pluronic is bound and covering the GO surface.[33] Additionally, two new absorption peaks formed at 2,890 cm^{-1} and 2,975 cm^{-1} that are characteristics of CH_2 and CH_3 functional groups, respectively.[34,35] However, the peak for CH_3 is barely noticeable and dominated by the peak for CH_2, which has a much higher intensity. This can be explained by referring to the basic chemical structure of Pluronic which shows the presence of only one CH_3 functional group for each Pluronic subunit, as can be seen in Figure 2B. The presence of these characteristic peaks confirms the functionalization of Pluronic onto GO samples.

XRD Analysis

Graphite shows a characteristic sharp peak at 2Θ degree of 26.5° that represents the diffraction of the (0 0 2) crystalline plane with the interlayer spacing of about 3.4 Å (Figure 3). This characteristic graphite peak disappeared in the XRD spectrum of GO, and a new GO characteristic peak appeared at about 2Θ degree of 9.81°, with the interlayer spacing of 9.01 Å. The increase in the interlayer spacing is probably due to the high degree of exfoliation[36] and intercalation of water molecules and oxygenated functional groups, such as carboxylic acid, hydroxyl groups, and epoxides between the hydrophilic GO layers.[37] A similar phenomenon was also observed for NanoGO, with the presence of a new characteristic peak at 2Θ degree of 9.31°, and a broadened interlayer spacing of 9.49 Å. The appearance of a broad strong characteristic peak in both the GO and NanoGO samples at 9.81° and 9.31°, respectively, indicates the successful formation of well exfoliated GO samples. The XRD spectra of both GO-PF and NanoGO-PF exhibited two sharp characteristic peaks at 2Θ degree of 23.33° and 19.19°, which correspond to the characteristic peaks of PF, thus confirming the functionalization of GO samples with PF through surface coating.

Field Emission Scanning Electron Microscopy (FESEM), EDX Analysis, and Transmission Electron Microscopy (TEM)

Field-emission scanning electron microscopy (FESEM) (FEI, USA) was employed to further elucidate the surface morphology and structure of the different GO aqueous dispersion samples. It was revealed in Figure 4A and B that the surface morphology of GO appeared as a wrinkled, thin film which is consistent with the previously reported morphology of GO as a large sheet with a rippled, silk-like surface.[37] Figure 4C and D, respectively, show the FESEM and TEM micrographs of NanoGO which is revealed to have a more porous topology resembling a loose sponge-like structure with perforations. This could be explained by the mechanical process of reducing the lateral dimension of GO sheets to nano-size GO particles through sonication, which causes the formation of smaller size GO nanosheets. This is postulated to cause the GO nanosheets to be more densely interlinked through overlapping and agglomeration between nanosheets, and subsequently forming a porous network.[38] Next, Figure 3D and E shows the GO-PF and NanoGO-PF, respectively. There were noticeable differences observed between these samples with GO, suggesting that Pluronic was successfully functionalized to the surface of GO-PF and NanoGO-PF. GO-PF appears to have a more wrinkled surface morphology, indicating alterations of the GO structure through Pluronic functionalization. Similarly,

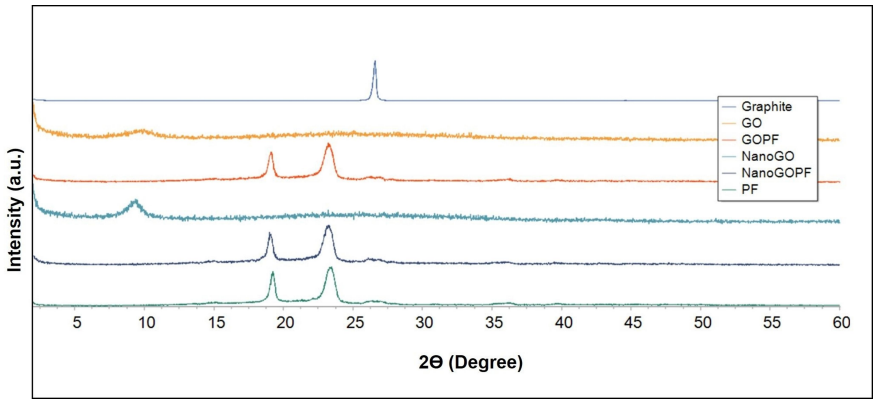

Figure 3 XRD patterns of pristine graphite, GO, GO-PF, NanoGO, and NanoGO-PF, along with PF as control measured at 30 kV and 30 mA, with a scanning rate of 2°/min and 2Θ angles ranging from 2–60°.

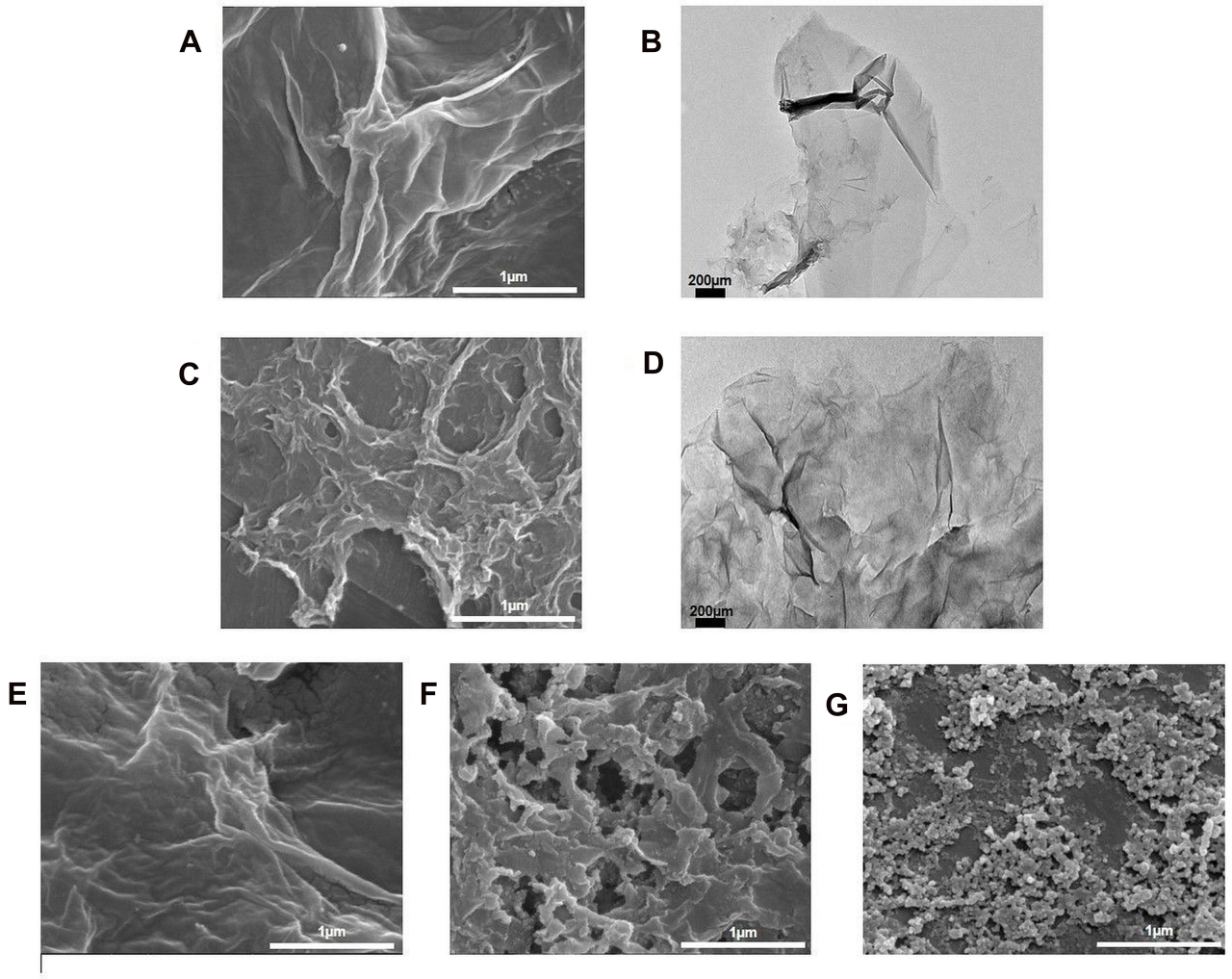

Figure 4 FESEM and TEM micrographs of: (**A**) GO; (**B**) GO (TEM); (**C**) NanoGO; (**D**) NanoGO (TEM); (**E**) GO-PF; and (**F**) NanoGO-PF dispersed in distilled water at 1 mg/mL, along with (**G**) PF as control. Scale bar shown is at 2 μm for FESEM micrographs and 200 nm for TEM micrographs.

the surface morphology of NanoGO-PF appears to have a less distinct porous structure as compared to NanoGO seen in Figure 4E, which is most likely to indicate the presence of Pluronic that is bound to the NanoGO surface, covering its sponge-like pores and forming a denser structure. In addition to that, GO-PF and NanoGO-PF show round micellar structures of Pluronic (Figure 4F).

Figure 5 shows the energy-dispersive X-ray (EDX) spectra of graphite, native GO samples (GO and NanoGO), functionalized GO samples (GO-PF and NanoGO-PF), and Pluronic F127. As shown in Table 2, the carbon, C element is present in a high percentage in pristine graphite (86.68%). The composition of oxygen increased significantly from 7.12% in pristine graphite to 43.63% and 32.92%, respectively, in GO and NanoGO, indicating the successful addition of oxygenated functional groups in GO and NanoGO during the process of synthesis. There were, however, amounts of silicon, Si (1.41% in GO), sulphur, S (4.36% in GO and 12.16% in NanoGO), and chloride (0.58% in GO and 2.69% in NanoGO), originating from the synthesis process and impurities present in the pristine graphite. A loss of oxygen-containing group during sonication is also observed in a study by Nam et al,[39] that utilized the zeta potential of GO suspension before and after sonochemical approach. This is in agreement with the present study, which shows an increase in the zeta potential of NanoGO to −47.408 when compared to GO (−53.042) (Figure 7C), that could be attributed by the lesser presence of an oxygen-containing group following 24 hours of sonication. Upon functionalization of Pluronic F127, the oxygen containing group in NanoGO-PF increases, together with the C composition, as Pluronic itself is composed of C and oxygen (O) elements. The impurities present in GO and

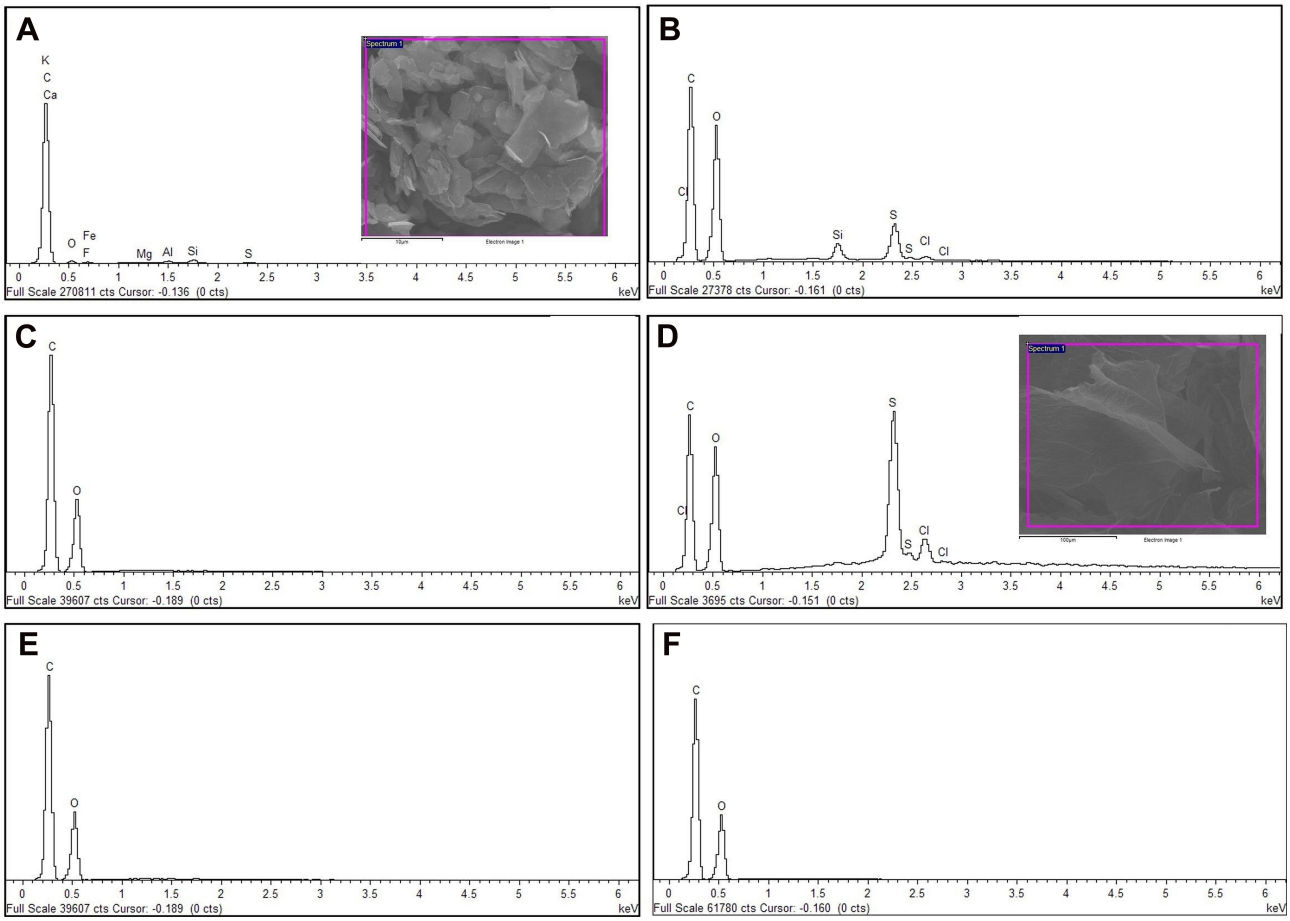

Figure 5 Energy-dispersive X-ray (EDX) spectra of (**A**) pristine graphite; (**B**) GO; (**C**) GO-PF; and (**D**) NanoGO; (**E**) NanoGO-PF, along with (**F**) PF as control.

NanoGO were completely removed when both samples were functionalized through surface coating with PF.

Ultraviolet-Visible (UV-Vis) Spectrophotometer

The characteristic feature of UV-Vis spectroscopy for all samples displays a strong absorption peak of GO at 228 nm corresponding to the $\pi \rightarrow \pi^*$ transition of C=C ring bonds and another shoulder at 300 nm corresponds to the $n \rightarrow \pi^*$ transition of the C=O bonds (Figure 6).[25,40,41] A UV-visible spectrum shows an upward shift and higher absorbance in the NanoGO than other GO samples. This could be attributed to the exfoliation of the GO sheets following 24 hours of sonication, which creates more particles that are able to absorb more light.[30] The optical absorption peak at 228 nm, originating from the π-plasmon of carbon,[42,43] remained unchanged in both GO and NanoGO. The UV-Vis spectrum for NanoGO-PF exhibited similar characteristics peak of GO and NanoGO.

Table 2 Elemental Analysis of All GO Samples, Pristine Graphite, and PF

Samples	C	O	F	Mg	Al	Si	S	K	Cl	Fe
Graphite	86.68	7.12	2.44	0.14	0.64	1.30	0.33	0.15	0.31	0.90
GO	50.19	43.63				1.41	4.36		0.58	
GO-PF	59.43	40.57								
NanoGO	52.24	32.92					12.16		2.69	
NanoGO-PF	59.36	40.64								
PF	53.80	46.12								

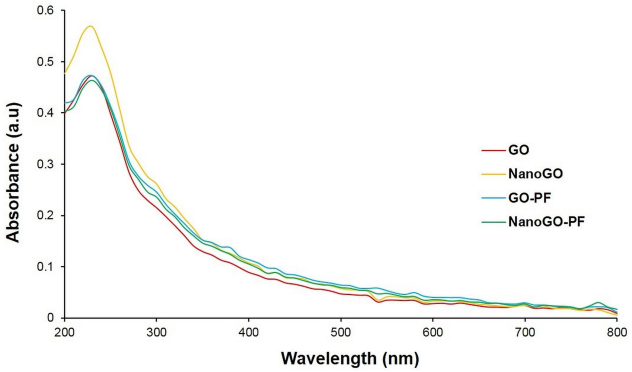

Figure 6 UV-Vis absorbance spectra of GO, NanoGO, GO-PF, and NanoGO-PF samples dispersed in distilled water at 1 mg/mL at 200–800 nm wavelengths.

Size, Size Distribution, and Zeta Potential Assessment

The preparation process of NanoGO was done in one step where the size of large GO sheets was reduced by sonication. The starting material, GO solution was made of large size exhibits HD of ~ 768.4 nm, PDI of 0.47, and a zeta potential of −46.41 mV (Figure 7). After the intense sonication, the HD size of larger GO sheets was reduced to an average size of 86.14 nm (Figure 7A). In addition, the NanoGO produced displays a negative zeta potential of −60.23 mV (Figure 7C). The NanoGO was well dispersed in deionized water and was very stable, showing no sign of aggregation and precipitation. The addition of non-ionic Pluronic onto NanoGO led to a significant increase of HD (~ 221.82 nm) and of the zeta potential (−10.52 mV). Coating of Pluronic masked the negative surfaces charges of the NanoGO which was observed by the increased zeta potential.[44] The addition of PF onto the large sheet of GO did not significantly increase the size of GO (Figure 7A), albeit an improved size distribution (Figure 7B) and increased zeta potential of GO-PF (Figure 7C). GO and NanoGO show a significant improvement in size distribution upon functionalization with Pluronic, which indicates good colloidal stability[45] and uniform dispersion. The hydrophobic part of Pluronic, PPO segment binds interacts with the hydrophobic part of the graphene oxide

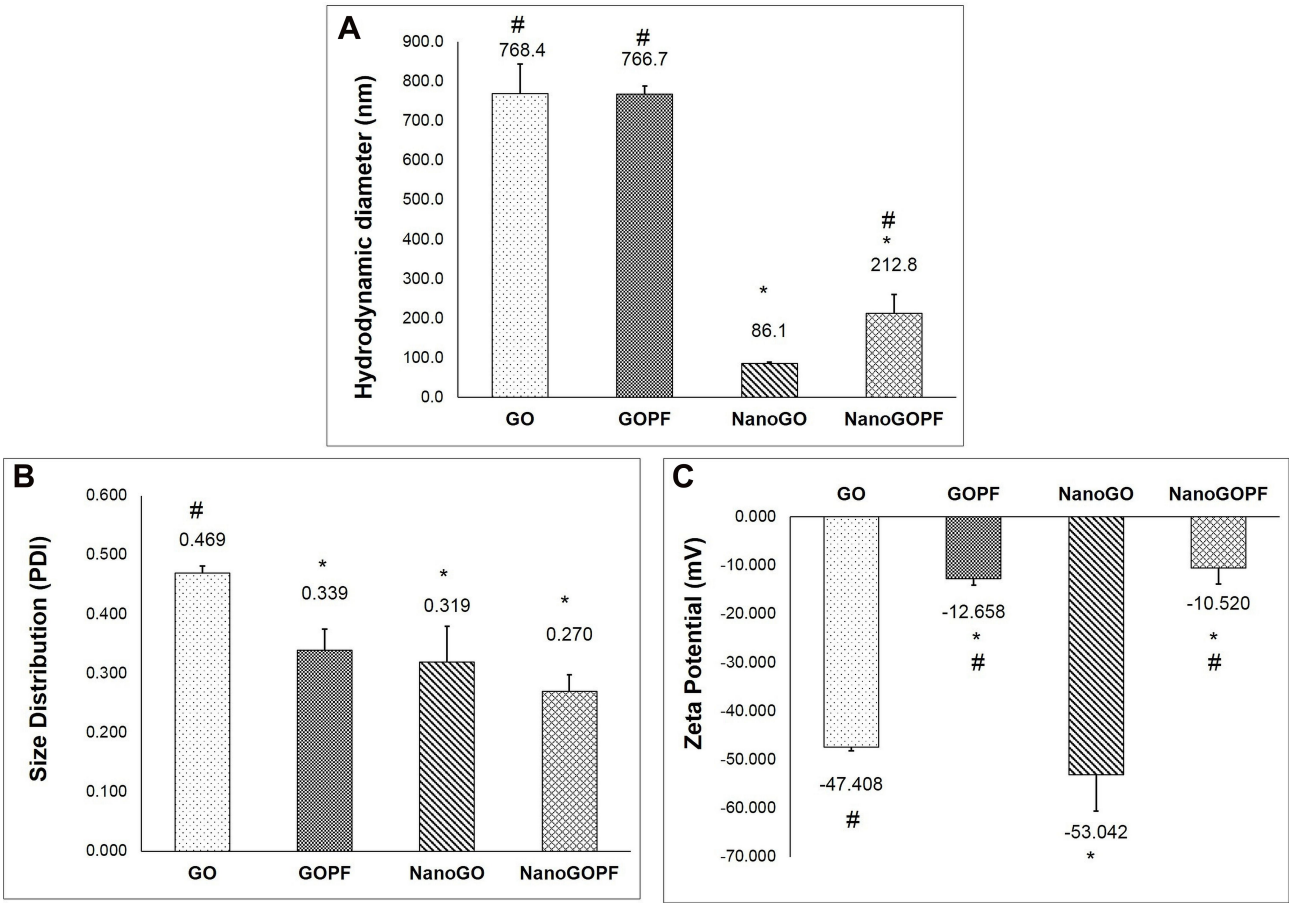

Figure 7 (**A**) Particle size, (**B**) size distribution, and (**C**) zeta potential of GO, GO-PF, NanoGO, and NanoGO-PF samples as measured by DLS. Data represents mean±SD (n>3). * Denotes significant difference compared to GO and # denotes significant difference compared to NanoGO, with $P \leq 0.05$.

sheet, while the hydrophilic segment that consists of PEO extends into the aqueous environment, providing an improved stability to the GO and NanoGO structure.[46,47]

Toxicity Assessment on Zebrafish Embryos

Survival Rate

One of the major hurdles in fully integrating GO application in industries, especially biomedicine, is the potential biocompatibility issues that have been reported in literature. There were many reports that suggest GO having significant cytotoxicity in both in vitro and in vivo studies involving various biological models such mammalian cells and animal models. However, functionalization of GO through surface coating has shown positive correlations between GO surface functionalization and reduced toxicity effect/improved toxicity profile. One of the many potential surface coatings that were studied was dextran (DEX), a type of glucose polymer, bovine serum albumin (BSA), and polyethylene glycol (PEG). A research group has reported that GO coated with DEX (GO-DEX) was highly biocompatible towards HeLa cell line, with cell viability remaining at 80%, even at concentrations of up to 450 μg/mL.[17] In addition, in vitro studies conducted using BSA as a surface coating on GO, have shown that it could improve GO biocompatibility, with only a slight inhibition towards cell proliferation up to 50 μg/mL. This was attributed to protein adsorption to GO, which weakened GO interaction towards the cells.[48,49] Besides that, another in vitro study also demonstrated that GO-PEG conjugate was highly biocompatible towards A549 cells, with no cytotoxicity response observed at concentrations of up to 100 μg/mL after a 48 hour incubation period.[50] Pluronic is of particular interest due to the fact that PEG, also known as polyethylene oxide (PEO), is one of the core components of the triblock copolymer. Thus, the fundamental properties of Pluronic as a surfactant and its ability to form micelles around particles could potentially prove useful for surface coating/functionalization in mitigating the toxicity effects of GO.

Pluronic (PF), also known as poloxamers, are non-ionic triblock copolymers composed of a central hydrophobic chain of polypropylene oxide (PPO) flanked by two hydrophilic chains of polyethylene oxide (PEO). Due to its amphiphilic structures, the polymers have surfactant properties that make it useful in industrial applications. Among other things, it can be used to increase the water solubility of hydrophobic, oily substances or otherwise increase the miscibility of two substances with different hydrophobic properties. For this same reason, these polymers are commonly used in industrial applications, cosmetics, and pharmaceuticals. Pluronic has also been evaluated for various drug delivery applications, such as the delivery of hydrophobic compound, curcumin,[51] and was even shown to sensitize drug-resistant cancers to chemotherapy.[52,53] In the present study, PF was non-covalently functionalized with GO, which involved a simple and efficient synthesis process.

Figure 8 shows the survival rate of zebrafish embryos treated with the test samples, with GO exhibiting the highest mortality rate. Starting with the GO-treated group, as shown in Figure 8A, the embryonic survival rate was at 100% among embryos in the control (CTRL) group, as well as at lower concentrations of GO from 1–5 μg/mL when observed up to 96 hpf. Although there was a slight decrease in survival rate for embryos treated with 10 and 15 μg/mL of GO, it was not significant when compared to control. However, starting from 30–60 μg/mL of GO, a significant decrease in the survival rate was seen at 48 hours, and the embryos have shown a continuous decline in the survival rate at the end of the exposure period (96 hpf). At the highest treatment concentrations of GO; 90 and 100 μg/mL, the survival rate of the GO-treated embryos declined drastically after 24 hpf, to 0% upon exposure period of 48 hpf. This finding elucidates that GO toxicity is dependent on the dosage and exposure period.[26,54,55] Based on Figure 8B, GO-PF exhibited the most promising results, demonstrating no decline in the survival rate at all concentrations (1–100 μg/mL) up to 96 hpf, albeit a slight decline in embryonic survival rate to 95.83% in 90–100 μg/mL of treatment groups at 72 hpf and a further noticeable decline to 87.5% at 96 hpf. However, it should be noted that this was not significant when compared to control.

As for the NanoGO-treated toxicity assay, similar to the toxicity profile observed in the GO-treated toxicity assay, the survival rate of embryos was also affected by the dosage and exposure period (Figure 8C). In NanoGO-treated embryos, lower concentrations of up to 15 μg/mL showed no significant decrease in survival rate, while at higher concentrations starting at 30 μg/mL, a significant decrease in survival rate was observed and experienced a further decline after prolonged exposure at 96 hpf. Interestingly, the embryonic mortality at higher concentrations of NanoGO (30–100 μg/mL) was not as drastic compared to GO. Although the survival

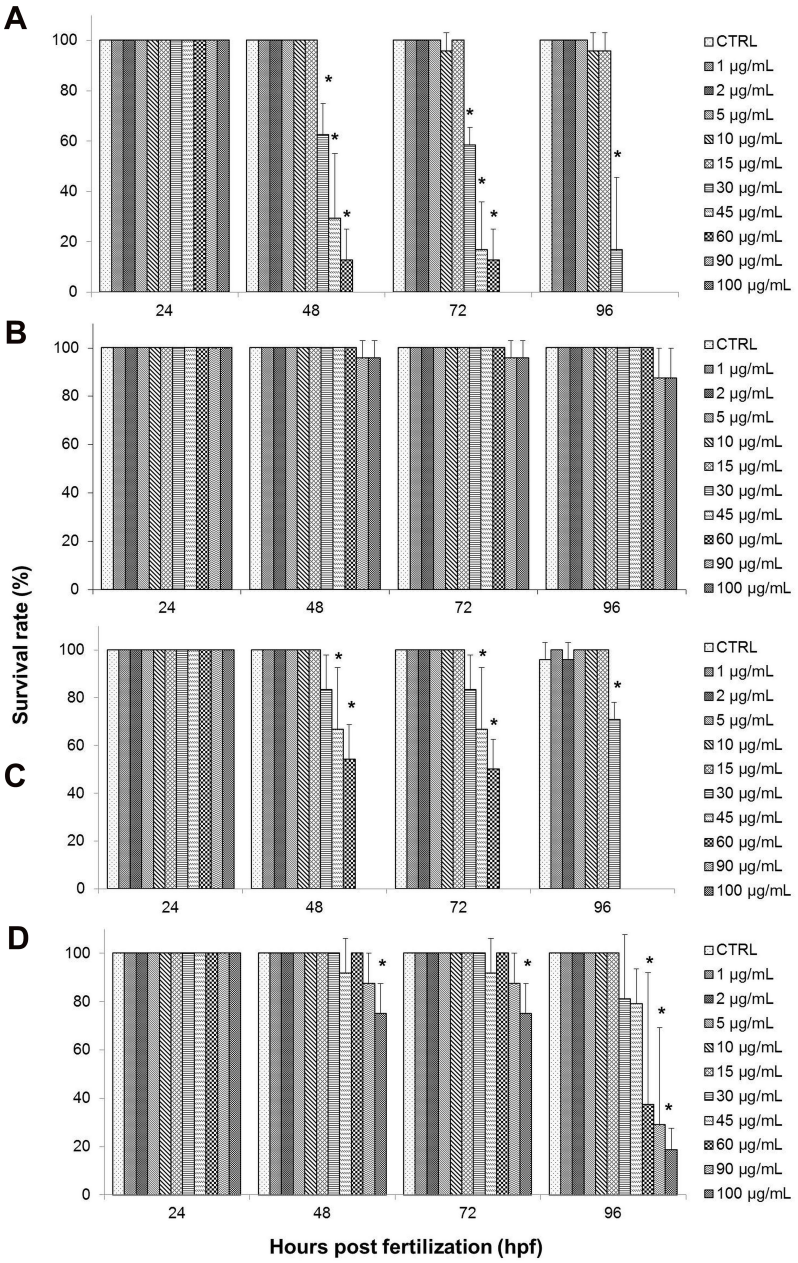

Figure 8 Effects of different treatments on survival of zebrafish (*Danio rerio*) embryos upon exposure at 24–96 hpf. Embryos of zebrafish were exposed at different concentrations of either (**A**) GO, (**B**) GO-PF, (**C**) NanoGO, or (**D**) NanoGO-PF at concentrations of 0–100 μg/mL. Distilled water was used as control. Data were averaged from three independent experiments and are shown as mean±SD. Significant difference compared to control treatment (CTRL) is denoted by "*" (One-way ANOVA, $P<0.05$).

rate at 90–100 μg/mL was comparable to GO, with a 0% survival rate at 48–96 hpf, the survival rate at 30–60 μg/mL improved significantly in NanoGO treated embryos, and was found to only experience a drastic decline at 96 hpf when compared to control, which demonstrated a somewhat delayed toxicological response in NanoGO-treated embryos. NanoGO exhibited a lower toxicity response toward the treated embryos compared to GO, which establish a size-dependent toxicity response by GO.

This finding is supported by several in vitro and in vivo studies that showed nano-sized GO possessed lower toxicity compared to micro-sized GO.[56,57] Lower toxicity of NanoGO could be due to the lesser interaction with immune cells, and subsequently interfere with the activation of NF-Kβ pathway and the production of inflammatory cytokines. Another possibility is because nano-sized GO is more likely to be eliminated through the excretory pathways. Unlikely, micro-sized GO is larger and it has

been reported to be accumulated in different organs, hence leading to a more rapid toxicity response.[14,58,59] Upon exposure of NanoGO to the embryo, it is quickly excreted out, causing it to take a longer time to accumulate in the embryo and induce toxic effects as elucidated by the delayed toxicity profile of NanoGO shown in Figure 8C. Large size GO with sharp edges interacts with the cells membrane and adhere to the embryonic chorion,[60] which in turns exacerbate the impacts on survival of the cells at the highest exposure dose, while small size GO induced significant cytotoxicity via internalization into the cells even at the lower concentration exposed.[61]

There was a significant improvement of the survival rate of the treated embryos when exposed to NanoGO-PF at similar concentrations (1–100 μg/mL) (Figure 8D). The embryonic survival rate was shown to decrease significantly at 75% in embryos treated with 100 μg/mL of NanoGO-PF upon exposure at 48 hpf, but with no further decline at 72 hpf. However, further decline was observed when embryos were exposed to the similar concentration of NanoGO-PF at 18.75% upon prolonged exposure at 96 hpf. Embryos treated with other concentrations of NanoGO-PF (1–45 μg/mL) did not show any significant decline in the survival rate throughout the exposure period of 96 hpf, which elucidate the ability of Pluronic to mitigate the toxicity of NanoGO in treated embryos. As for the survival rate of NanoGO-PF-treated embryos, shown in Figure 6D, there was also marked improvement when compared against NanoGO. Embryonic survival rate only decreased significantly in 100 μg/mL at 48 hpf, while other concentrations of 60 μg/mL and 90 μg/mL experienced significant decline at 96 hpf. This again demonstrates the dose–effect and time–effect relationship of NanoGO-PF toxicity, which is evidenced by the toxicity profile described above. NanoGO exhibited lower toxicity compared to GO, which establishes a size-dependent toxicity response by GO.[62] However, NanoGO-PF, on the other hand, demonstrated a higher toxicity profile compared to GO-PF, as seen in Figure 8B and C, respectively. This contradictory finding is postulated to be caused by the lower amount of bound/functionalized Pluronic in NanoGO-PF in comparison to GO-PF. This could explain the decrease in survival rates of treated zebrafish embryos only after extended exposure to NanoGO-PF. Some of the surface of NanoGO was not properly coated with Pluronic surfactant, possibly due to the poor interaction with the porous, sponge-like surface morphology of NanoGO (Figure 6D), which enables the non-functionalized region of the NanoGO surface to interact with zebrafish embryos, and subsequently induce toxicity response.

Heart Rate

Heart rate was also one of the toxicological end-points in zebrafish development that was evaluated following exposure to GO samples. This was done to assess for any signs of cardiac disruption that might indicate potential toxicity effects. Transparent embryos during early stages of development allow for direct visual inspection of the heart morphology, as well as easy assessment of the heart rate.[63] Normal cardiac rhythm is vital for proper development and growth of zebrafish. The normal embryonic heart rate of zebrafish is measured at 120–180 beats per minute (bpm), which is closer to the normal human heart rate compared to conventional animal models such as mouse.[64,65] Heart rate was expressed as the heartbeat measurements of the surviving embryos in different concentrations and exposure periods.

There was no significant decrease in the heart rate of zebrafish embryos after being treated to GO, as well as NanoGO based on the findings exhibited in Figure 9A and C. No significant signs of bradycardia (slow heartbeat) or tachycardia (fast heartbeat) was observed throughout the assessment period of up to 96 hpf for any of the treatment concentrations when compared to the respective control groups. However, there was a noticeable decrease in heartbeat in 60 μg/mL of GO, which is an outlier due to the fact that only one embryo survived at that concentration.

Contrary to the observations for GO and NanoGO treated embryos, a significant decrease in heart rate was exhibited in embryos treated with GO-PF at the highest treatment concentration, 100 μg/mL at 48 hpf and 72 hpf (Figure 9B). Finally, embryos exposed to 60 and 90 μg/mL of NanoGO-PF showed a significant decrease in heart rate ($P<0.05$), as seen in Figure 9D only after 96 hpf. The presence of Pluronic F127 as dispersant for GO has also shown to increase the degree of lactate dehydrogenase (LDH) leakage in THP-1 cells exposed to 80 and 100 μg/mL of single layer GO (SLGO).[66] The increased level of ROS[64] and degree of LDH leakage in GO samples functionalized with Pluronic could potentially contribute to the decreased heart rate observed in embryos treated with GO-PF and NanoGO-PF samples, which requires further investigation. In another study conducted by Ain et al,[67] PEG-nGO administered intraperitoneally in mice at the concentration of 5 mg/kg had significantly increased the concentration of malondialdehyde (MDA) in the heart to 330% compared to control

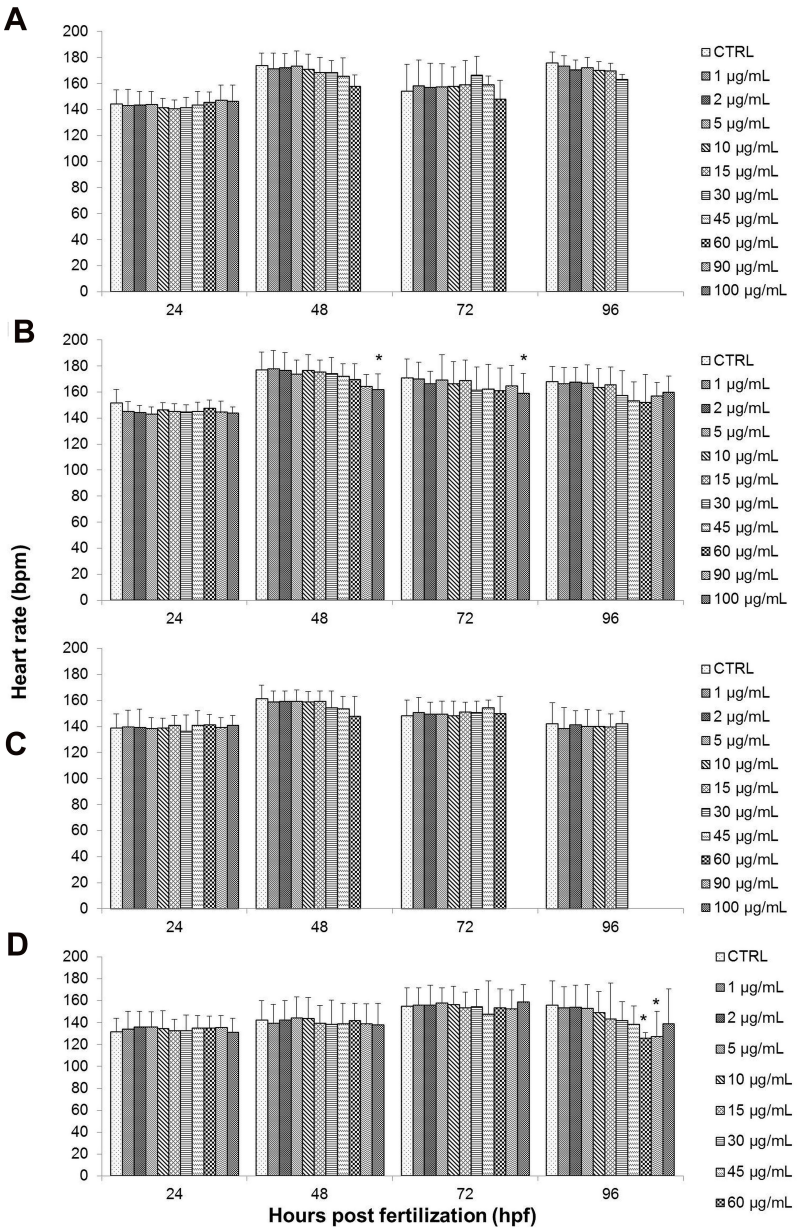

Figure 9 Effects of different treatments on the heart rate of zebrafish (*Danio rerio*) embryos upon exposure at 24–96 hpf. Embryos of zebrafish were exposed at different concentrations of either (**A**) GO, (**B**) GO-PF, (**C**) NanoGO, or (**D**) NanoGO-PF at concentrations of 0–100 µg/mL. Distilled water was used as control. Data were averaged from three independent experiments and are shown as mean±SD. Significant difference compared to control treatment (CTRL) is denoted by "*" (One-way ANOVA, $P<0.05$).

mice that received saline solution. This indicates that functionalization of GO with polymer, such as PEG, could possibly lead to an increase in the radical oxygen species (ROS) when administered, which could be detrimental to the vital organs, such as the heart.

Hatching Rate

Another end-point parameter that was observed was hatching rate. Hatching rate was also expressed as the percentage of hatched embryos after exposure to different concentrations of toxicant, as seen in Figure 8. Embryonic hatching usually occurs between 48 hpf and 72 hpf during normal zebrafish development and is seen as a critical stage in zebrafish embryogenesis.[68,69]

Based on the results of the present study, GO and NanoGO exposure did not exhibit any significant effect on the hatching rate of treated embryos compared to the respective control groups, as shown in Figure 8A and C, respectively. GO-treated embryos experienced 100% hatching rate at almost all treatment concentrations.

However, a slight decline in hatching rate to 96% was observed for the control group and at 1 and 2 µg/mL, while a drop to 88% in hatching rate was observed at 10 µg/mL. Similarly, embryos exposed to NanoGO at 48 hpf also experienced a slight decrease in hatching rate at 2, 5, and 10 µg/mL, as well as control group, with only a 92% hatching rate while the hatching rate at 1 µg/mL was at 88%.

The embryonic hatching rate was also not significantly affected by exposure to GO-PF and NanoGO-PF. Figure 10 and D, respectively, show the hatching rates of GO-PF and NanoGO-PF-treated zebrafish embryos which were comparable to the embryonic hatching rates during GO and NanoGO treatment (Figure 10A and C). Embryonic hatching rate in GO-PF toxicity assay experienced a decline at 48 hpf in 1, 5, 45, and 60 µg/mL, as well as in the control group that was not significant ($P<0.05$). NanoGO-PF also demonstrated a decrease in hatching rate in 5, 15, and 45 µg/mL at 48 hpf. Interestingly, the decline in embryonic hatching rate in 45 µg/mL to 96% was observed up to 72 hpf, indicating an incidence of permanent delayed-hatching involving one zebrafish embryo, which is not significant ($P<0.05$) when compared to control. The findings obtained in the present study are in agreement with a study conducted by Liu et al,[26] which observed no noticeable and significant effect to hatching rate of zebrafish when exposed to a similar concentration range of GO concentration (0, 1, 5, 10, 50, and 100 mg/L).

Morphological Assessment

Another important parameter used in zebrafish toxicity assay to evaluate the toxicity effects of GO samples was morphological assessment. This was performed to assess for any abnormalities induced by GO toxicity during zebrafish embryogenesis. Malformations that were assessed in the present study include pericardial edema (PE), yolk sac edema (YSE), scoliosis (SC), non-detachment of tail, and lack of somite formation. The results obtained from the toxicity assay showed no significant increase in the incidence of malformations when exposed to different concentrations of GO up to 96 hpf. GO toxicity assay showed no malformation incidence such as edema and scoliosis. Only one embryo incubated in 30 µg/mL of NanoGO exhibited incidence of PE at 96 hpf, which is not significant when compared to control. GO and NanoGO showed no other abnormalities including non-detachment of tail and lack of somite formation. It is also worth noting that only the occurrence of PE was detected, while YSE malformation was not observed in any of the toxicity assays that were conducted.

Similarly, the toxicity assay of GO-PF and NanoGO-PF samples detected no significant increase in the malformation incidence throughout the exposure period. We reported no incidence of non-detachment of the tail as well as a lack of somite formations for all treatment concentrations up to 96 hpf. However, in GO-PF and NanoGO-PF treated toxicity assays, the occurrence of morphological abnormalities, especially edema, increased slightly compared to GO and NanoGO samples. NanoGO-PF showed a higher frequency of malformation occurrence, including PE and SC compared to GO-PF. Aside from that, as mentioned previously, all incidences of malformations observed were not significant when compared to control, indicating that Pluronic functionalization through surface coating does not significantly cause morphological defects during critical developmental stages in zebrafish embryos. Incidences of malformation that were observed such as PE and SC in zebrafish embryonic toxicity assay are shown in Figure 11, with the presence of PE and SC indicated by an asterisk and black triangular icon, respectively. Figure 11 also shows the normal embryonic development of zebrafish from 24 to 96 hpf, with visible changes in morphology during different stages of growth.

Further in vivo administration of Pluronic-functionalized GO in other model organisms, such as rats that reflects more on the human intrauterine environment is warranted to investigate the bioavailability and biodistribution profiles of Pluronic-functionalized GO in the maternal blood and embryos, respectively. A recent study by Cherian et al[70] has observed the biodistribution of rGO-P in the brain, liver, spleen, kidney, bone marrow, and blood of the dams following intravenous administration of 10 mg/kg of rGO-P in a Wistar rat model, which suggested possible feto–placental transmission. The bioavailability of this rGO-P was, however, only analyzed qualitatively, using Raman spectroscopy.

Conclusion

In the present study, different GO samples were prepared and characterized before further use in zebrafish toxicity assay to evaluate the dose-, time-, and size-dependent toxicity effects on zebrafish embryonic development. Aside from that, the potential of GO surface functionalization to mitigate toxicological response by utilizing Pluronic surfactant as a surface coating was also explored. The Pluronic-functionalized GO samples were assessed

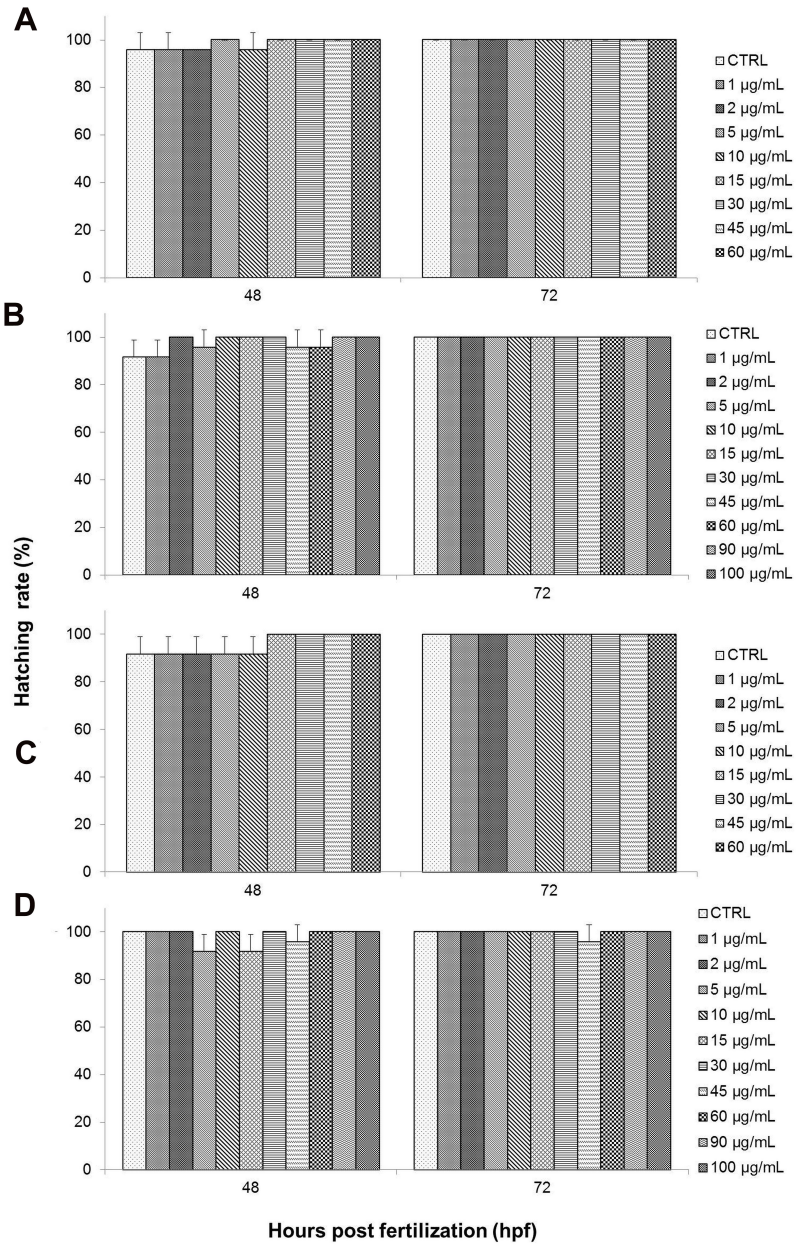

Figure 10 Hatching rate (%) of zebrafish (*Danio rerio*) embryos exposed to different treatments of either (**A**) GO, (**B**) GO-PF, (**C**) NanoGO, or (**D**) NanoGO-PF at concentrations of 0–100 µg/mL. Distilled water was used as control. Data were expressed as mean±SD. No significant delay was observed between experimental groups.

using zebrafish embryo to compare against native (non-functionalized) GO samples. Characterization of the different GO samples that was conducted using DLS, Raman spectroscopy, UV-Vis, FTIR, and FESEM analyses has successfully identified and validated the structural and chemical properties along with the surface morphology of all the GO samples with respect to previous findings. Based on the toxicity assay performed, it was observed that the toxicological response of GO samples exhibited a dose- and time-dependent relationship. Size or lateral dimension also influenced the toxicity effects of GO samples as evidenced by the comparatively better toxicity profile of NanoGO against GO. Besides effects on embryonic mortality, there was no other significant alteration to the hatching rate or morphology of the treated zebrafish embryos when compared against respective control groups. Lastly, this study shows a remarkable improvement to the GO toxicity as elucidated by the survival rate of GO-PF, as well as NanoGO-PF. GO-PF, and NanoGO-PF have, however, induced heart rate

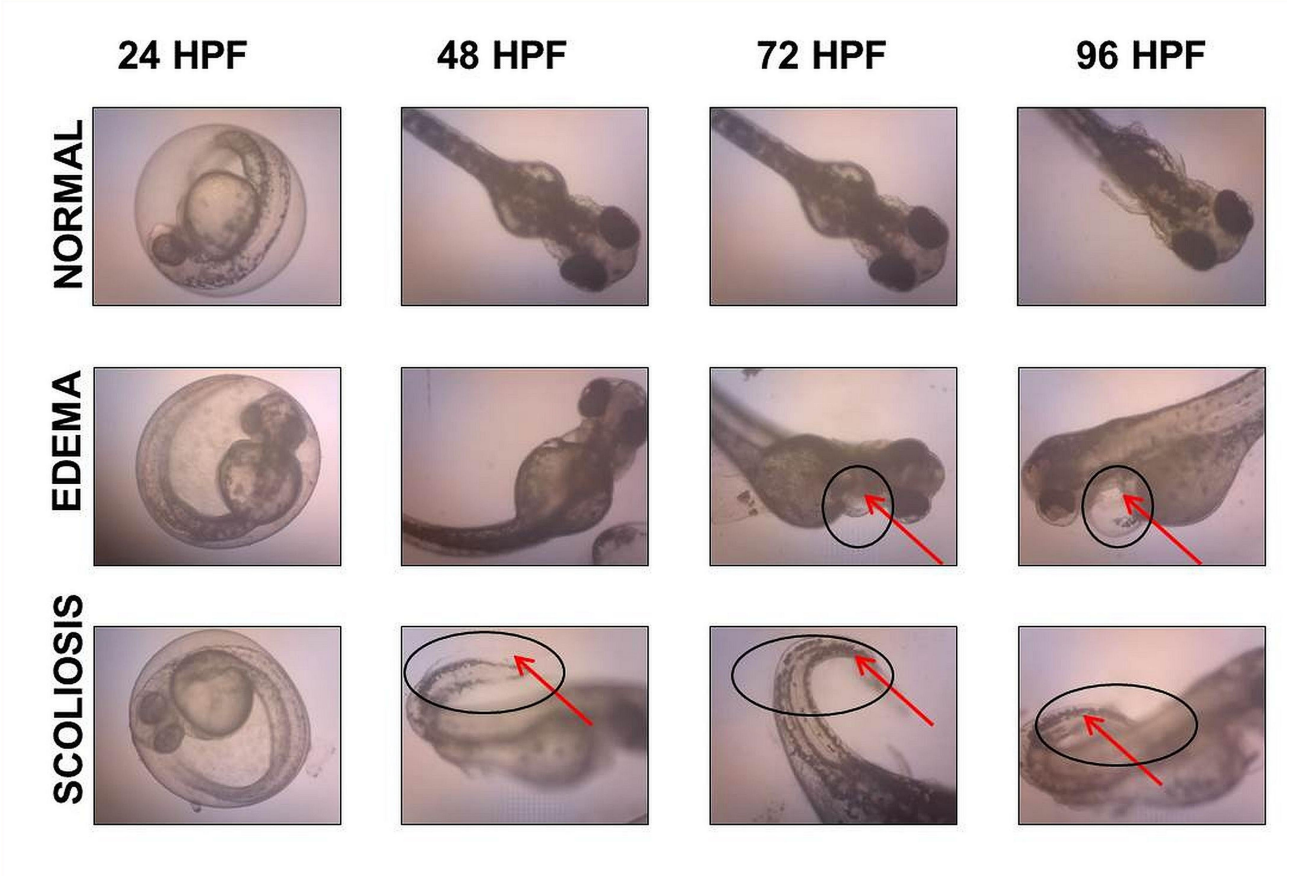

Figure 11 Microscope images showing incidence of malformations in zebrafish embryo, including PE and SC, as indicated by a black circle and arrow.

induction in zebrafish embryos at higher concentrations, which warrants further investigation. The present study highlighted the potential of Pluronic F127 to improve the biocompatibility and toxicological response of GO, but the long-term effect of Pluronic F127 has to be thoroughly investigated for future development in the clinical settings.

Funding

This research was funded by research grants from Ministry of Higher Education of Malaysia, namely Fundamental Research Grant Scheme (FRGS), grant number 04-01-18-1931FR and Universiti Putra Malaysia (GP/IPM/2016/9513200). Authors acknowledge the facilities, scientific and technical assistance from the Institute of Advanced Technology (ITMA) and Institute of Biosciences (IBS) at Universiti Putra Malaysia.

Disclosure

The authors report no conflicts of interest in this work.

References

1. Sheshmani S, Fashapoyeh MA. Suitable chemical methods for preparation of graphene oxide, graphene and surface functionalized graphene nanosheets. *Acta Chim Slov*. 2013;60:813–825.
2. Pan Y, Sahoo NG, Li L. The application of graphene oxide in drug delivery. *Expert Opin Drug Del*. 2012;9(11):1365–1376. doi:10.1517/17425247.2012.729575
3. Yuan W, Zhou Y, Li Y, et al. The edge- and basal-plane-specific electrochemistry of a single-layer graphene sheet. *Sci Rep*. 2013;3(1):2248. doi:10.1038/srep02248
4. Goenka S, Sant V, Sant S. Graphene-based nanomaterials for drug delivery and tissue engineering. *J Control Release*. 2014;173:75–88. doi:10.1016/j.jconrel.2013.10.017
5. Gao Y, Wu J, Ren X, et al. Impact of graphene oxide on the antibacterial activity of antibiotics against bacteria. *Environ Sci Nano*. 2017;4(5):1016–1024. doi:10.1039/C7EN00052A
6. Hou WC, Lee PL, Chou YC, Wang YS. Antibacterial property of graphene oxide: the role of phototransformation. *Environ Sci Nano*. 2017;4(3):647–657. doi:10.1039/C6EN00427J
7. Shamsi S, Elias N, Sarchio SNE, Yasin FM. Gallic acid loaded graphene oxide based nanoformulation (GAGO) as potential anti-bacterial agent against Staphylococcus aureus. *Mater Today*. 2018;5(January):S160–165.
8. Liu CW, Xiong F, Jia HZ, et al. Graphene-based anticancer nanosystem and its biosafety evaluation using a Zebrafish model. *Biomacromolecules*. 2013;14(2):358–366. doi:10.1021/bm3015297

9. Yang X, Wang Y, Huang X, et al. Multi-functionalized graphene oxide based anticancer drug-carrier with dual-targeting function and pH-sensitivity. *J Mater Chem*. 2011;21(10):3448–3454. doi:10.1039/C0JM02494E
10. Zhang L, Xia J, Zhao Q, Liu L, Zhang Z. Functional graphene oxide as a nanocarrier for controlled loading and targeted delivery of mixed anticancer drugs. *Small*. 2010;6(4):537–554. doi:10.1002/smll.200901680
11. Gurunathan S, Arsalan Iqbal M, Qasim M, et al. Evaluation of graphene oxide induced cellular toxicity and transcriptome analysis in human embryonic kidney cells. *Nanomaterials (Basel)*. 2019;9(7):E969. doi:10.3390/nano9070969
12. Gurunathan S, Kang MH, Jeyaraj M, Kim JH. Differential cytotoxicity of different sizes of graphene oxide nanoparticles in leydig (TM3) and sertoli (TM4) cells. *Nanomaterials (Basel)*. 2019;9(2):E139. doi:10.3390/nano9020139
13. Wen KP, Chen YC, Chuang CH, Chang HY, Lee CY, Tai NH. Accumulation and toxicity of intravenously-injected functionalized graphene oxide in mice. *J Appl Toxicol*. 2015;35(10):1211–1218. doi:10.1002/jat.3187
14. Zhang XY, Yin J, Peng C, et al. Distribution and biocompatibility studies of graphene oxide in mice after intravenous administration. *Carbon*. 2011;49(3):986–995. doi:10.1016/j.carbon.2010.11.005
15. Xu M, Zhu J, Wang F, et al. Improved in vitro and in vivo biocompatibility of graphene oxide through surface modification: poly (acrylic acid)-functionalization is superior to PEGylation. *ACS Nano*. 2016;10(3):3267–3281. doi:10.1021/acsnano.6b00539
16. Liu F, Yang D, Liu Y, et al. Improving dispersive property, biocompatibility and targeting gene transfection of graphene oxide by covalent attachment of polyamidoamine dendrimer and glycyrrhetinic acid. *Colloids Surf B Biointerfaces*. 2018;171:622–628. doi:10.1016/j.colsurfb.2018.07.067
17. Kim YK, Kim MH, Min DH. Biocompatible reduced graphene oxide prepared by using dextran as a multifunctional reducing agent. *ChemComm*. 2011;47(11):3195–3197.
18. Zhang X, Yang R, Wang C, Heng CL. Cell biocompatibility of functionalized graphene oxide. *Acta Physico-Chimica Sinica*. 2012;28(6):1520–1524. doi:10.3866/PKU.WHXB201203131
19. Ma M, Cheng L, Zhao A, Zhang H, Zhang A. Pluronic-based graphene oxide-methylene blue nanocomposite for photodynamic/photothermal combined therapy of cancer cells. *Photodiagnosis Photodyn Ther*. 2020;29:101640. doi:10.1016/j.pdpdt.2019.101640
20. Karahan HE, Wei L, Goh K, et al. Synergism of water shock and a biocompatible block copolymer potentiates the antibacterial activity of graphene oxide. *Small*. 2016;12:951. doi:10.1002/smll.201502496
21. Fako VE, Furgeson DY. Zebrafish as a correlative and predictive model for assessing biomaterial nanotoxicity. *Adv Drug Deliv Rev*. 2009;61:478–486. doi:10.1016/j.addr.2009.03.008
22. Wiecinski PN, Metz KM, Heiden TCK, Louis KM, Mangham AN, Hamers RJ. Toxicity of oxidatively degraded quantum dots to developing zebrafish (Danio rerio). *Environ Sci Techno*. 2013;47:9132–9139. doi:10.1021/es304987r
23. Sant KE, Timme-Laragy AR. Zebrafish as a model for toxicological perturbation of yolk and nutrition in the early embryo. *Curr Environ Health Rep*. 2018;5:125–133. doi:10.1007/s40572-018-0183-2
24. Marcano DC, Kosynkin DV, Berlin JM, et al. Improved synthesis of graphene oxide. *ACS Nano*. 2010;4(8):4806–4814. doi:10.1021/nn1006368
25. Hu H, Yu J, Li Y, Zhao J, Dong H. Engineering of a novel Pluronic F127/graphene nanohybrid for pH responsive drug delivery. *J Biomed Mater Res A*. 2012;100A(1):141–148. doi:10.1002/jbm.a.33252
26. Liu XT, Mu XY, Wu XL, et al. Toxicity of multi-walled carbon nanotubes, graphene oxide, and reduced graphene oxide to zebrafish embryos. *Biomed Environ Sci*. 2014;27(9):676–683.
27. Pylatiuk C, Sanchez D, Mikut R, et al. Automatic zebrafish heartbeat detection and analysis for zebrafish embryos. *Zebrafish*. 2014;11(4):379–383. doi:10.1089/zeb.2014.1002
28. Gao J, Liu F, Liu Y, Ma N, Wang Z, Zhang X. Environment-friendly method to produce graphene that employs vitamin C and amino acid. *Chem Mater*. 2010;22(7):2213–2218. doi:10.1021/cm902635j
29. Makharza S, Cirillo G, Bachmatiuk A, Vittorio O. Size-dependent nanographene oxide as a platform for efficient carboplatin release. *J Mater Chem B*. 2013;1:6107–6114. doi:10.1039/c3tb21090a
30. Le GTT, Chanlek N, Manyam J, et al. Insight into the ultrasonication of graphene oxide with strong changes in its properties and performance for adsorption applications. *Chem Eng J*. 2019;373:1212–1222. doi:10.1016/j.cej.2019.05.108
31. Dos Santos MSC, Gouvêa AL, de Moura LD, et al. Nanographene oxide-methylene blue as phototherapies platform for breast tumor ablation and metastasis prevention in a syngeneic orthotopic murine model. *J Nanobiotechnology*. 2018;16(9):1–17. doi:10.1186/s12951-018-0333-6
32. Jang S, Oh Y, Vilian ATE, et al. Nano-graphene oxide composite for in vivo imaging. *Int J Nanomedicine*. 2018;13:221–234. doi:10.2147/IJN.S148211
33. Li B, Zhang L, Zhang Z, et al. Physiologically stable F127-GO supramolecular hydrogel with sustained drug release characteristic for chemotherapy and photothermal therapy. *RSC Adv*. 2018;8(3):1693–1699. doi:10.1039/C7RA12099K
34. Dissanayaket L, Frech R. Infrared spectroscopic study of the phases and phase transitions in poly(ethylene oxide) and poly(ethylene oxide)-lithium trifluoromethanesulfonate complexes. *Macromolecules*. 1995;28(15):5312–5319. doi:10.1021/ma00119a022
35. Muthoosamy K, Abubakar IB, Bai RG, Loh H. Exceedingly higher co-loading of curcumin and paclitaxel onto polymer-functionalized reduced graphene oxide for highly potent synergistic anticancer treatment. *Sci Rep*. 2016;6:32808. doi:10.1038/srep32808
36. Ouyang Y, Cai X, Shi Q, et al. Poly-L-lysine-modified reduced graphene oxide stabilizes the copper nanoparticles with higher water-solubility and long-term additively antibacterial activity. *Colloids Surf B Biointerfaces*. 2013;107:107–114. doi:10.1016/j.colsurfb.2013.01.073
37. Dorniani D, Saifullah B, Barahuie F, et al. Graphene oxide-gallic acid nanodelivery system for cancer therapy. *Nanoscale Res Lett*. 2016;11(1):491–498. doi:10.1186/s11671-016-1712-2
38. Bera M, Gupta P, Maji PK. Facile one-pot synthesis of graphene oxide by sonication assisted mechanochemical approach and its surface chemistry. *J Nanosci Nanotechnol*. 2018;18(2):902–912. doi:10.1166/jnn.2018.14306
39. Nam SW, Jung C, Li H, et al. Adsorption characteristics of diclofenac and sulfamethoxazole to graphene oxide in aqueous solution. *Chemosphere*. 2015;136:20–26. doi:10.1016/j.chemosphere.2015.03.061
40. Gurunathan S, Han JW, Dayem AA, Eppakayala V, Kim JH. Oxidative stress-mediated antibacterial activity of graphene oxide and reduced graphene oxide in Pseudomonas aeruginosa. *Int J Nanomedicine*. 2012;7:5901–5914. doi:10.2147/IJN.S37397
41. Some S, Gwon A-R, Hwang E, et al. Cancer therapy using ultrahigh hydrophobic drug-loaded graphene derivatives. *Sci Rep*. 2015;4(1):6314. doi:10.1038/srep06314
42. Attal S, Thiruvengadathan R, Regev O. Determination of the concentration of single-walled carbon nanotubes in aqueous dispersions using UV - Visible absorption spectroscopy. *Anal Chem*. 2006;78(23):8098–8104. doi:10.1021/ac060990s
43. Reed BW, Sarikaya M. Electronic properties of carbon nanotubes by transmission electron energy-loss spectroscopy. *Phys Rev B*. 2001;64:195404. doi:10.1103/PhysRevB.64.195404
44. Sahu A, Choi WI, Lee JH, Tae G. Graphene oxide mediated delivery of methylene blue for combined photodynamic and photothermal therapy. *Biomaterials*. 2013;34:6239–6248. doi:10.1016/j.biomaterials.2013.04.066
45. Cherian RS, Sandeman S, Ray S, Savina IN, Ashtami J, Mohanan PV. Green synthesis of Pluronic stabilized reduced graphene oxide: chemical and biological characterization. *Colloids Surf B Biointerfaces*. 2019;179:94–106. doi:10.1016/j.colsurfb.2019.03.043

46. Li S, Guo J, Patel RA, Dadlani AL, Leblanc RM. Interaction between graphene oxide and Pluronic F127 at the air-water interface. *Langmuir*. 2013;29(19):5742–5748. doi:10.1021/la401056t
47. Zu S-Z, Zan B-H. Aqueous dispersion of graphene sheets stabilized by pluronic copolymers: formation of supramolecular hydrogel. *J Phys Chem C*. 2009;113(31):13651–13657. doi:10.1021/jp9035887
48. Cheng C, Nie S, Li S, et al. Biopolymer functionalized reduced graphene oxide with enhanced biocompatibility via mussel inspired coatings/anchors. *J Mater Chem B*. 2013;1(3):265–275. doi:10.1039/C2TB00025C
49. Mu Q, Su G, Li L, et al. Size-dependent cell uptake of protein-coated graphene oxide nanosheets. *ACS Appl Mater*. 2012;4(4):2259–2266. doi:10.1021/am300253c
50. Xu Z, Zhu S, Wang M, Li Y, Shi P, Huang X. Delivery of paclitaxel using PEGylated graphene oxide as a nanocarrier. *ACS Appl Mater Interfaces*. 2015;7:1355–1363. doi:10.1021/am507798d
51. Shamsi S, Chen Y, Lim LY. Characterization and biological properties of NanoCUR formulation and its effect on major human cytochrome P450 enzymes. *Int J Pharm*. 2015;495(1):194–203. doi:10.1016/j.ijpharm.2015.08.066
52. Wang M, Wu J, Li Y, et al. A tumor targeted near-infrared light-controlled nanocomposite to combat with multidrug resistance of cancer. *J Control Release*. 2018;288:34–44. doi:10.1016/j.jconrel.2018.08.037
53. Xu C, Xu J, Zheng Y, et al. Active-targeting and acid-sensitive pluronic prodrug micelles for efficiently overcoming MDR in breast cancer. *J Mater Chem B*. 2020;8(13):2726–2737. doi:10.1039/C9TB02328C
54. Chen LQ, Hu PP, Zhang L, Huang SZ, Luo LF, Huang CZ. Toxicity of graphene oxide and multi-walled carbon nanotubes against human cells and zebrafish. *Sci China Chem*. 2012;55(10):2016–2209. doi:10.1007/s11426-012-4620-z
55. Ghafor AAHA, Elias N, Shamsi S, Yasin FM, Sarchio SNES. Toxicity assessment of gallic acid loaded graphene oxide (GAGO) nano-formulation in zebrafish (Danio rerio) embryos. *Pertanika J Sci Tech*. 2020;28(1):311–326.
56. Yue H, Wei W, Yue Z, et al. The role of the lateral dimension of graphene oxide in the regulation of cellular responses. *Biomaterials*. 2012;33(16):4013–4021. doi:10.1016/j.biomaterials.2012.02.021
57. Zhang H, Peng C, Yang J, et al. Uniform ultrasmall graphene oxide nanosheets with low cytotoxicity and high cellular uptake. *ACS Appl Mater Interfaces*. 2013;5(5):1761–1767. doi:10.1021/am303005j
58. Ma J, Liu R, Wang X, et al. Crucial role of lateral size for graphene oxide in activating macrophages and stimulating pro-inflammatory responses in cells and animals. *ACS Nano*. 2015;9(10):10498–10515. doi:10.1021/acsnano.5b04751
59. Wang K, Ruan J, Song H, et al. Biocompatibility of graphene oxide. *Nanoscale Res Lett*. 2011;6(1):8–15.
60. Chen Z, Yu C, Khan IA, Tang Y, Liu S, Yang M. Toxic effects of different-sized graphene oxide particles on zebrafish embryonic development. *Ecotoxicol Environ Saf*. 2020;197:110608. doi:10.1016/j.ecoenv.2020.110608
61. Jia P-P, Sun T, Junaid M, et al. Nanotoxicity of different sizes of graphene (G) and graphene oxide (GO) in vitro and in vivo. *Environ Pollut*. 2019;247::595–606. doi:10.1016/j.envpol.2019.01.072
62. Verkerk AO, Remme CA. Zebrafish: a novel research tool for cardiac (patho)electrophysiology and ion channel disorders. *Front Physiol*. 2012;3:255–263. doi:10.3389/fphys.2012.00255
63. Baker K, Warren KS, Yellen G, Fishman MC. Defective "pacemaker" current (Ih) in a zebrafish mutant with a slow heart rate. *Proc Natl Acad Sci U S A*. 1997;94:4554–4559. doi:10.1073/pnas.94.9.4554
64. De Luca E, Zaccaria G, Hadhoud M, et al. ZebraBeat: a flexible platform for the analysis of the cardiac rate in zebrafish embryos. *Sci Rep*. 2015;4:4898. doi:10.1038/srep04898
65. Cho YC, Pak PJ, Joo YH, Lee HS, Chung N. In vitro and in vivo comparison of the immunotoxicity of single- and multi-layered graphene oxides with or without Pluronic F-127. *Sci Rep*. 2016;6:38884. doi:10.1038/srep38884
66. Cherian RS, Anju S, Paul W, Sabareeswaran A, Mohanan PV. Organ distribution and biological compatibility of surface-functionalized reduced graphene oxide. *Nanotechnology*. 2020;31(7):075303.
67. Ain QT, Haq SH, Alshammari A, Al-Mutlaq MA, Anjum MN. The systemic effect of PEG-nGO-induced oxidative stress in vivo in a rodent model. *Beilstein J Nanotechnol*. 2019;10:901–911. doi:10.3762/bjnano.10.91
68. d'Amora M, Camisasca A, Lettieri S, Giordani S. Toxicity assessment of carbon nanomaterials in zebrafish during development. *Nanomaterials (Basel, Switzerland)*. 2017;7(12):414–425. doi:10.3390/nano7120414
69. Kimmel CB, Ballard WW, Kimmel SR, Ullmann B, Schilling TF. Stages of embryonic development of the zebrafish. *Dev Dynam*. 1995;203(3):253–310. doi:10.1002/aja.1002030302
70. Cherian RS, Anju S, Paul W, Sabareeswaran A, Mohanan PV. Organ distribution and biological compatibility of surface-functionalized reduced graphene oxide. *Nanotechnology*. 2020;31:075303.